Imaging the distribution of photoswitchable probes with temporally-unmixed multispectral optoacoustic tomography

X. Luís Deán-Ben, Andre C. Stiel, Yuanyuan Jiang, Vasilis Ntziachristos, Gil G. Westmeyer and Daniel Razansky

Institute for Biological and Medical Imaging, Technical University of Munich and Helmholtz Center Munich, Ingolstädter Landstraße 1, 85764 Neuherberg, Germany.

ABSTRACT

Synthetic and genetically encoded chromo- and fluorophores have become indispensable tools for biomedical research enabling a myriad of applications in imaging modalities based on biomedical optics. The versatility offered by the optoacoustic (photoacoustic) contrast mechanism enables to detect signals from any substance absorbing light, and hence these probes can be used as optoacoustic contrast agents. While contrast versatility generally represents an advantage of optoacoustics, the strong background signal generated by light absorption in endogeneous chromophores hampers the optoacoustic capacity to detect a photo-absorbing agent of interest. Increasing the optoacoustic sensitivity is then determined by the capability to differentiate specific features of such agent. For example, multispectral optoacoustic tomography (MSOT) exploits illuminating the tissue at multiple optical wavelengths to spectrally resolve (unmix) the contribution of different chromophores. Herein, we present an alternative approach to enhance the sensitivity and specificity in the detection of optoacoustic contrast agents. This is achieved with photoswitchable probes that change optical absorption upon illumination with specific optical wavelengths. Thereby, temporally unmixed MSOT (tuMSOT) is based on photoswitching the compounds according to defined schedules to elicit specific time-varying optoacoustic signals, and then use temporal unmixing algorithms to locate the contrast agent based on their particular temporal profile. The photoswitching kinetics is further affected by light intensity, so that tuMSOT can be employed to estimate the light fluence distribution in a biological sample. The performance of the method is demonstrated herein with the reversibly switchable fluorescent protein Dronpa and its fast-switching fatigue resistant variant Dronpa-M159T.

Keywords: Optoacoustic imaging, photoswitchable proteins, Dronpa, Dronpa-M159T, temporally unmixed multispectral optoacoustic tomography.

1. INTRODUCTION

Synthetic as well as genetically encoded chromo- and fluorophores are essential tools for biomedical research and diagnostics enabling a large range of applications *in vitro* and *in vivo*.[1] Dedicated imaging instrumentation is used to distinguish specific absorbing or fluorescent contrast agents from background signals based on their absorbance or fluorescence spectrum. This is typically done by means of optical filters that extract a small bandwidth of the spectrum of the contrast agent of interest, in a way that multiple filters covering a large portion of the optical spectrum can be employed to increase the contrast-to-noise ratio (CNR) associated to the distribution of the contrast agent.[2,3]

On the other hand, optoacoustic (photoacoustic) imaging enables breaking the light diffusion limit for resolving optical contrast in biological tissues with much higher resolution than optical techniques, thus offering new *in vivo* insights that growingly attract interest of the biomedical research community.[4–7] In more detail, the conversion of light to mechanical waves (optoacoustic effect) is mediated by the local absorption of photons and nonradiative relaxation of the absorbers, which results in thermal energy and thermoelastic expansion. Thereby, optoacoustic contrast can e.g. be provided by fluorophores such as well-established dyes or genetically encoded fluorescent proteins,[8,9] and a larger contrast versatility is further enabled by a myriad of probes and genetic reporters absorbing light photons.[10–12] The sensitivity in the detection of molecules for light intensities below

*E-mail: dr@tum.de, [a] Equal contribution, [b] Equal contribution

Photons Plus Ultrasound: Imaging and Sensing 2016, edited by Alexander A. Oraevsky, Lihong V. Wang
Proc. of SPIE Vol. 9708, 970825 · © 2016 SPIE · CCC code: 1605-7422/16/$18 · doi: 10.1117/12.2213459

the safety exposure limit is ultimately conditioned by the ultrasound measuring technology, being significantly lower than in fluorescence imaging systems. More importantly, the strong background signal generated by light absortion in endogeneous chromophores hampers the optoacoustic capacity to detect the photo-absorbing agent of interest. Increasing the optoacoustic senstivity is then determined by the capability to differentiate specific features of such agent. In this way, multispectral optoacoustic tomography (MSOT) exploits illuminating the tissue at multiple optical wavelengths to spectrally resolve (unmix) the contribution of different chromophores.[13–15]

Specificity in the absorption properties is also present in a special subset of chromo- and fluorophores that change their photo-physical properties as a function of incident light. For example, reversibly switchable fluorescent proteins (RSFPs) can be reversibly switched between a fluorescent and a non-fluorescent state.[16] These photoresponsive chromo- and fluorophores have been used in tracking schemes and single molecule studies or in so-called super-resolution microscopy techniques that enable fluorescence imaging well beyond the diffraction limit.[17]

Herein, we describe an alternative exploitation of the photoswitching capability of specific compounds to enhance the sensitivity and specificity of optoacoustics imaging. This is achieved by photoswitching the compounds according to defined sequences of optical wavelengths to create specific time-varying optoacoustic signals, so that temporal unmixing algorithms are subsequently used to locate the contrast agent based on its particular temporal profile. On the other hand, the switching kinetics can further be exploited for light fluence normalization. Optoacoustic images are proportional to the light fluence distribution, which can have variations higher than an order of magnitude for millimeter- to centimeter-scale depths. Several procedures based on theoretical models, iterative methods or multispectral approaches have been suggested for light fluence normalization.[18–21] For photoswitchable probes, the activation and deactivation time constants are a function of the number of incident photons and hence depend on the light fluence distribution. Thereby, herein we take advantage of the spatial dependence of the temporal profiles to propose a method to correct for the light fluence distribution in optoacoustic images, so that tuMSOT can potentially be used as a quantitative molecular imaging tool.

2. MATERIALS AND METHODS

2.1 Experimental setup

The experimental system employed is depicted in Fig. 1a. A spherical array of 256 piezocomposite detectors was used to provide a three-dimensional optoacoustic image of a sample with each laser pulse, so that an imaging rate determined by the pulse repetition frequency of the laser is achieved.[22] A mutant version of the photoswitchable protein Dronpa (Dronpa-M159T) as well as the wild-type protein were used in the experiments. The imaging sample was immersed in water to guarantee acoustic coupling. An optical parametric oscillator (OPO)-based laser was used as an illumination source. The laser wavelength can be tuned in the range 420-710 nm in a per pulse basis, so that a sequence of arbitrary wavelengths in this range can be generated at the pulse repetition frequency of the laser (50 Hz). For activation and deactivation of the protein, the wavelength was switched between 420 and 488 nm as indicated in Fig. 1b.

2.2 Temporal unmixing

Assuming a stochastic process, the number of active molecules for a given instant $N(t)$ can be expressed as

$$N(t) = N_0 e^{-\alpha t}, \tag{1}$$

where N_0 is the number of initially activated molecules and α is the photoswitching rate. Under the same environmental parameters such as temperature, viscosity and pH, α is proportional to the light fluence, i.e., $\alpha = k\Phi$, being k a constant that depends on the photoswitching kinetics of a specific substance and on the optical wavelength employed. Considering that the optoacoustic signal intensity $p(t)$ is similarly proportional to the number of activated molecules, its temporal dependence can be expressed as

$$p(t) = p_0 e^{-k\Phi t}, \tag{2}$$

p_0 being the initial optoacoustic signal rendered with the probe in its fully activated state. Both Eqs. 1 and 2 are expressed as a function of time t, which in our particular case represents number of excitation laser pulses.

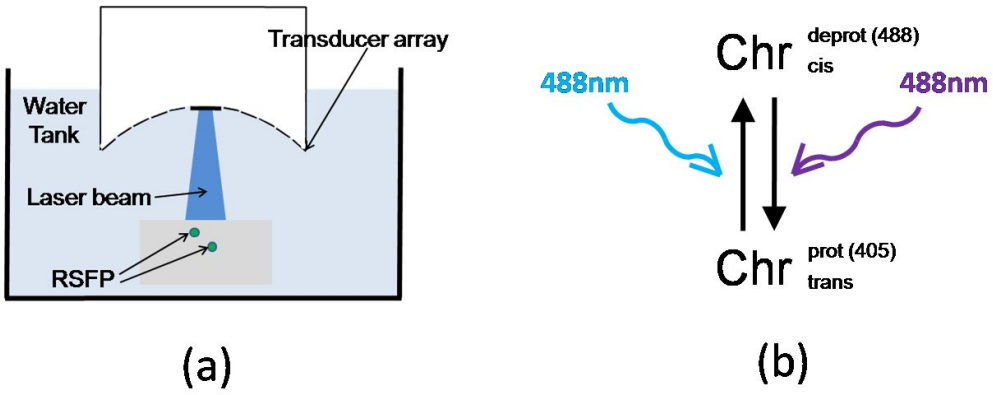

Figure 1. (a) Lay-out of the experimental system to image the reversible switchable fluorescent proteins (RSFP). (b) Photophysical properties of Dronpa and Dronpa-M159T, depicting the switching modes of the proteins and the excitation wavelengths employed for switching.

The time profile associated to the optoacoustic signal generated by the probe can be distinguished from the constant optoacoustic signal generated by background components. Thereby, an unmixing algorithm can be employed to estimate the distribution of the probe as explained in Ref. 23.

2.3 Light fluence estimation

As mentioned in the previous section, the time constant α is proportional to the light fluence so that the light fluence distribution can be estimated from a sequence of optoacoustic images. For this, the actual measured temporal profiles of the optoacoustic signal at different locations in the images were fitted to an exponential-like curve $y(t)$ in the form of

$$y(t) = a_1 e^{-b_1 t} + a_2 e^{-b_2 t}. \tag{3}$$

In Eq. 3, the light fluence is assumed to be proportional to b_1. The second term in Eq. 3 was included to account for the residual signal in the tubing for the deactivated protein as well as for potential slow variations associated to laser fluctuations, temperature changes, bleaching and other parameters. More details are provided in Ref. 24.

3. RESULTS

In a first experiment, three tubigs were embedded in agar containing blood, Dronpa and the mutant version Dronpa-M159T respectively. The resulting optoacoustic image obtained for 488 nm excitation for the fully activated proteins is displayed in Fig. 2a. The tubings containing the proteins are not visible in this image due to the strong signal generated at the tubing containing blood. Image unmixing was performed from a sequence of images were wavelengths 488 nm and 420 nm were alternated. Fig. 2b shows the unmixed distributions of the wild-type and mutant proteins obtained with an unmixing algorithm termed vertex component analysis (VCA).[25,26] The temporal profiles for 488 nm excitation are also displayed. This unmixing algorithm allows isolating the contribution of both proteins even for a signal level which is orders of magnitude lower than that of blood. Standard unmixing with least square fitting to the time profiles obtained at specific points in the tubings can also be used for temporal unmixing (Fig. 2c), although the sensitivity is lower with this procedure as manifested in the cross-talk noise present in the images.

In a second experiment, two tubings were embedded in an agar phantom containing Intralipid to mimic optical scattering in biological tissues. In this way, light attenuation is produced, so that the optoacoustic signal for the tubing at a deeper location is lower than that for the other tubing containing the same concentration of the protein. This is shown in the three dimensional view in Fig. 2d. This image was normalized with the estimated decay rate inside the tubings, yielding the image displayed in Fig. 2e. The intensity of the signal at

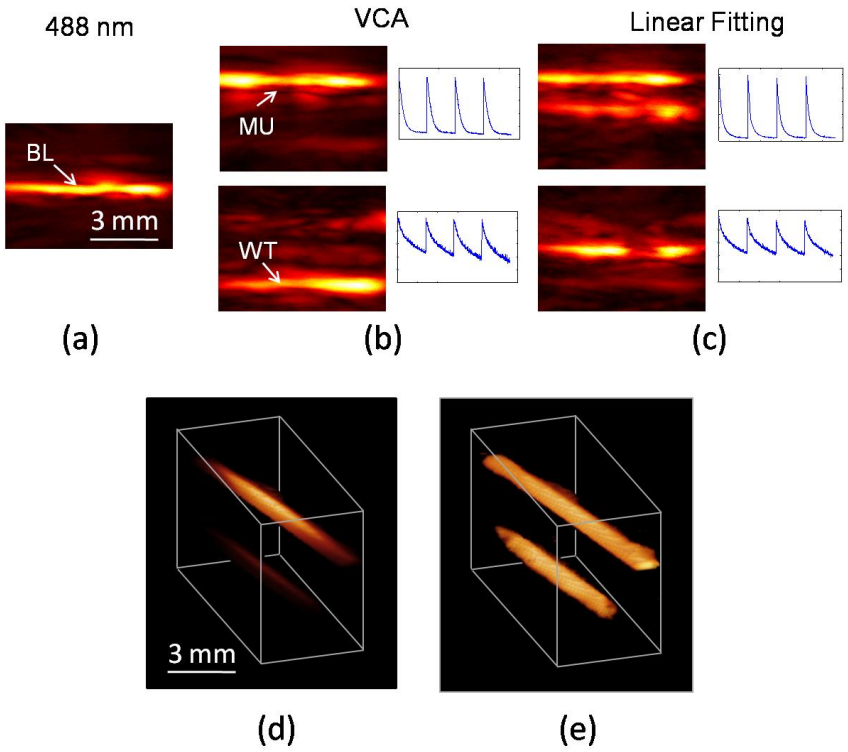

Figure 2. (a) Maximum intensity projection of the three-dimensional optoacoustic image for an agar phantom with three tubings containing blood (BL), wild-type Dronpa (WT), and the mutant protein Dronpa-M159T (MU) when both proteins are fully activated. (b) Unmixed distributions of Dronpa and Dronpa-M159T obtained with vertex component analysis along with the temporal profiles for 488 nm. (c) Unmixed distributions of Dronpa and Dronpa-M159T obtained with least square fitting along with the temporal profiles for 488 nm. (d) Three-dimensional image of an agar phantom with Intralipid containing two tubings at different depths with Dronpa-M159T. (e) Equivalent image after normalizing with the estimated decay rates inside the tubings.

both tubings in the normalized image is approximately the same,[24] which indicates a good performance of the suggested method for light fluence normalization.

4. CONCLUSIONS

The feasility of generating specific optoacoustic temporal profiles by photoswitching molecules was shown herein, for which a fast-wavelength-tuning short-pulsed laser operating in the visible region of the spectrum was used. The capabililty of the laser to tune the optical wavelength in a per-pulse basis can further be exploited to generate multispectral profiles in a very short time.[27] Specifically, the reversibly switchable fluorescent proteins Dronpa and its fast-switching fatigue resistant variant Dronpa-M159T were used. Optoacoustic imaging experiments further demonstrate the ability to temporally unmix proteins with identical spectra and strong background absorbers such as blood.

On the other hand, the presented results showcase the basic feasibility to correct for the light fluence distribution in biological tissues by accounting for changes in the time deactivation constant of photoswitchable probes. The photoswitchable fluorescent protein Dronpa-M159T used herein is a very convenient probe for this purpose as it is fatigue resistant and rapidly switchable. Since the deactivation cycle can be repeated in a very short time for the fast-switching Dronpa-M159T, dynamic imaging of the distribution of this agent is enabled provided high-frame rate acquisition is performed,[22] where the temporal resolution is generally given by the time required for the activation-deactivation cycle. The development of probes for tuMSOT, particularly for near-

infrared wavelengths,[28] represents an important challenge to address. In this range of the spectrum, tuMSOT may potentially be used for quantitative molecular imaging with a very high sensitivity.

ACKNOWLEDGMENTS

Acknowledgment. A. C. S. would like to thank Birte Hoecker for constant support and for the opportunity to conduct the protein biochemistry work in her laboratory. G. G. W. acknowledges support by Technische Universitaet Muenchen, the Helmholtz Association of German Research Centers, and Helmholtz Alliance ICEMED. Funding from the European Research Council (ERC) (ERC-2010-StG-260991, ERC-2012-StG-311552) is acknowledged.

REFERENCES

[1] Weissleder, R. and Pittet, M. J., "Imaging in the era of molecular oncology," *Nature* **452**(7187), 580–589 (2008).

[2] Hillman, E. M., "Optical brain imaging in vivo: techniques and applications from animal to man," *Journal of biomedical optics* **12**(5), 051402–051402 (2007).

[3] Themelis, G., Yoo, J. S., and Ntziachristos, V., "Multispectral imaging using multiple-bandpass filters," *Optics letters* **33**(9), 1023–1025 (2008).

[4] Mallidi, S., Kim, S., Karpiouk, A., Joshi, P. P., Sokolov, K., and Emelianov, S., "Visualization of molecular composition and functionality of cancer cells using nanoparticle-augmented ultrasound-guided photoacoustics," *Photoacoustics* **3**(1), 26–34 (2015).

[5] Gottschalk, S., Fehm, T. F., Deán-Ben, X. L., and Razansky, D., "Noninvasive real-time visualization of multiple cerebral hemodynamic parameters in whole mouse brains using five-dimensional optoacoustic tomography," *Journal of Cerebral Blood Flow & Metabolism* (2015).

[6] Heijblom, M., Piras, D., Brinkhuis, M., Van Hespen, J., Van den Engh, F., Van der Schaaf, M., Klaase, J., van Leeuwen, T., Steenbergen, W., and Manohar, S., "Photoacoustic image patterns of breast carcinoma and comparisons with magnetic resonance imaging and vascular stained histopathology," *Scientific reports* **5** (2015).

[7] Ermolayev, V., Dean-Ben, X. L., Mandal, S., Ntziachristos, V., and Razansky, D., "Simultaneous visualization of tumour oxygenation, neovascularization and contrast agent perfusion by real-time three-dimensional optoacoustic tomography," *European radiology* , 1–9 (2015).

[8] Krumholz, A., Shcherbakova, D. M., Xia, J., Wang, L. V., and Verkhusha, V. V., "Multicontrast photoacoustic in vivo imaging using near-infrared fluorescent proteins," *Scientific reports* **4** (2014).

[9] Deliolanis, N. C., Ale, A., Morscher, S., Burton, N. C., Schaefer, K., Radrich, K., Razansky, D., and Ntziachristos, V., "Deep-tissue reporter-gene imaging with fluorescence and optoacoustic tomography: a performance overview," *Molecular Imaging and Biology* **16**(5), 652–660 (2014).

[10] Jathoul, A. P., Laufer, J., Ogunlade, O., Treeby, B., Cox, B., Zhang, E., Johnson, P., Pizzey, A. R., Philip, B., Marafioti, T., et al., "Deep in vivo photoacoustic imaging of mammalian tissues using a tyrosinase-based genetic reporter," *Nature Photonics* (2015).

[11] Kirscher, L., Deán-Ben, X. L., Scadeng, M., Zaremba, A., Zhang, Q., Kober, C., Fehm, T. F., Razansky, D., Ntziachristos, V., Stritzker, J., et al., "Doxycycline inducible melanogenic vaccinia virus as theranostic anti-cancer agent," *Theranostics* **5**(10), 1045 (2015).

[12] Jiang, Y., Sigmund, F., Reber, J., Deán-Ben, X. L., Glasl, S., Kneipp, M., Estrada, H., Razansky, D., Ntziachristos, V., and Westmeyer, G. G., "Violacein as a genetically-controlled, enzymatically amplified and photobleaching-resistant chromophore for optoacoustic bacterial imaging," *Scientific reports* **5** (2015).

[13] Taruttis, A., Wildgruber, M., Kosanke, K., Beziere, N., Licha, K., Haag, R., Aichler, M., Walch, A., Rummeny, E., and Ntziachristos, V., "Multispectral optoacoustic tomography of myocardial infarction," *Photoacoustics* **1**(1), 3–8 (2013).

[14] Deán-Ben, X. L., Bay, E., and Razansky, D., "Functional optoacoustic imaging of moving objects using microsecond-delay acquisition of multispectral three-dimensional tomographic data," *Scientific reports* **4** (2014).

[15] Tzoumas, S., Deliolanis, N., Morscher, S., and Ntziachristos, V., "Unmixing molecular agents from absorbing tissue in multispectral optoacoustic tomography," *Medical Imaging, IEEE Transactions on* **33**(1), 48–60 (2014).

[16] Shcherbakova, D. M., Sengupta, P., Lippincott-Schwartz, J., and Verkhusha, V. V., "Photocontrollable fluorescent proteins for superresolution imaging," *Annual review of biophysics* **43**, 303 (2014).

[17] Nienhaus, K. and Nienhaus, G. U., "Fluorescent proteins for live-cell imaging with super-resolution," *Chemical Society Reviews* **43**(4), 1088–1106 (2014).

[18] Cox, B. T., Arridge, S. R., Köstli, K. P., and Beard, P. C., "Two-dimensional quantitative photoacoustic image reconstruction of absorption distributions in scattering media by use of a simple iterative method," *Applied Optics* **45**(8), 1866–1875 (2006).

[19] Jetzfellner, T., Rosenthal, A., Buehler, A., Englmeier, K.-H., Razansky, D., and Ntziachristos, V., "Multispectral optoacoustic tomography by means of normalized spectral ratio," *Optics letters* **36**(21), 4176–4178 (2011).

[20] Guo, Z., Hu, S., and Wang, L. V., "Calibration-free absolute quantification of optical absorption coefficients using acoustic spectra in 3d photoacoustic microscopy of biological tissue," *Optics letters* **35**(12), 2067–2069 (2010).

[21] Deán-Ben, X. L., Buehler, A., Razansky, D., and Ntziachristos, V., "Estimation of optoacoustic contrast agent concentration with self-calibration blind logarithmic unmixing," *Physics in medicine and biology* **59**(17), 4785 (2014).

[22] Deán-Ben, X. L., Ford, S. J., and Razansky, D., "High-frame rate four dimensional optoacoustic tomography enables visualization of cardiovascular dynamics and mouse heart perfusion," *Scientific reports* **5** (2015).

[23] Stiel, A. C., Deán-Ben, X. L., Jiang, Y., Ntziachristos, V., Razansky, D., and Westmeyer, G. G., "High-contrast imaging of reversibly switchable fluorescent proteins via temporally unmixed multispectral optoacoustic tomography," *Optics letters* **40**(3), 367–370 (2015).

[24] Deán-Ben, X. L., Stiel, A. C., Jiang, Y., Ntziachristos, V., Westmeyer, G. G., and Razansky, D., "Light fluence normalization in turbid tissues via temporally unmixed multispectral optoacoustic tomography," *Optics letters* **40**(20), 4691–4694 (2015).

[25] Deán-Ben, X. L., Deliolanis, N. C., Ntziachristos, V., and Razansky, D., "Fast unmixing of multispectral optoacoustic data with vertex component analysis," *Optics and Lasers in Engineering* **58**, 119–125 (2014).

[26] Nascimento, J. M. and Dias, J. M. B., "Vertex component analysis: A fast algorithm to unmix hyperspectral data," *Geoscience and Remote Sensing, IEEE Transactions on* **43**(4), 898–910 (2005).

[27] Deán-Ben, X. L. and Razansky, D., "Adding fifth dimension to optoacoustic imaging: volumetric time-resolved spectrally enriched tomography," *Light: Science & Applications* **3**(1), e137 (2014).

[28] Yao, J., Kaberniuk, A. A., Li, L., Shcherbakova, D. M., Zhang, R., Wang, L., Li, G., Verkhusha, V. V., and Wang, L. V., "Multiscale photoacoustic tomography using reversibly switchable bacterial phytochrome as a near-infrared photochromic probe," *Nature methods* (2015).